

Hierarchy of correlations for the Ising model in the Majorana representation

Álvaro Gómez-León

*Department of Physics and Astronomy and Pacific Institute of Theoretical Physics
University of British Columbia, 6224 Agricultural Rd., Vancouver, B.C., V6T 1Z1, Canada.*

(Dated: September 11, 2018)

We study the quantum Ising model in D dimensions with the equation of motion technique and the Majorana representation for spins. The decoupling scheme used for the Green's functions is based on the hierarchy of correlations in position space. To lowest order, this method reproduces the well known mean field phase diagram and critical exponents. When correlations between spins are included, we show how the appearance of thermal fluctuations and magnons strongly affect the physical properties. In 1D and for $B = 0$ we demonstrate that, to first order in correlations, thermal fluctuations completely destroy the ordered phase. For non vanishing transverse field we show that the model exhibits different behavior than its classical counterpart, specially near the quantum critical point. We discuss the connection with the Dyson's equation formalism and the explicit form of the self-energies.

Contents

Introduction	1
I. Method	2
II. Uncorrelated solution	3
III. Correlations in absence of transverse field	5
IV. Correlations in the Quantum Ising model	8
V. Conclusions	11
References	11
A. Correlated part of the 4-point function	12
B. Classical Ising model	13

Introduction

The transverse Ising model corresponds to one of the most studied systems in quantum physics. One reason is the large number of physical effects that can be described within this model: Ferromagnetic/Paramagnetic (FM/PM) transitions¹, spin glass phases^{2,3}, frustration⁴, many-body localization⁵, etc. Besides its theoretical interest, it also models a large variety of real systems, such as interacting magnetic molecules^{6,7}, coupled superconducting circuits and many others whose low energy description consists on coupled two-level systems. In addition, the understanding of the Ising system is very important for quantum computation; for example, finding the ground state of the spin glass phase corresponds to an NP problem⁸, which is typically used to benchmark quantum annealers^{9,10}. Furthermore, the 2D Ising model in a transverse field corresponds to a universal Hamiltonian¹¹ which can be used to effectively describe many other models. Related to all the previous interests, recent the studies on the dynamical properties of the

Ising model^{12,13}, or on the effect of decoherence^{14–16} show how the physics is even richer than previously thought.

The equation of motion technique in combination with the hierarchy of correlations represent a useful non-perturbative approach to understand the consequences of correlations in many-body system^{17–20}. When it is used to describe real space correlations, it corresponds to the well known $1/\mathcal{Z}$ expansion, \mathcal{Z} being the coordination number of the lattice; however, it can also be generalized to e.g., correlations between momentum space modes, providing an alternative scaling which can improve the convergence under some circumstances²¹. The main idea is to separate the correlation functions into uncorrelated and correlated parts; here the first part describes the single particle physics, while the second corresponds to collective excitation effects. The usefulness of this separation becomes clear when one finds a scaling for the correlated part, as a function of the physical parameters. This allows to organize terms hierarchically, in terms of decreasing contributions to the correlation functions.

In this work we analyze the transverse field Ising model in D dimensions, using the hierarchy of correlations in position space. We discuss the advantages and limitations of the method by comparing with some well established results, and show that, as expected by the increase of the coordination number with D , the scaling of real spatial correlations improves with the dimension of the system. We also discuss the critical exponents and the properties of the phase transitions in this model.

The work is organized as follows: In section I we introduce the Majorana representation and the basic idea behind a hierarchy of correlations. In section II we discuss the uncorrelated solution of the Quantum Ising model and discuss its advantages and limitations. In section III we include the effect of correlations in absence of a transverse field, which allows for a simpler discussion of the method, and a direct comparison with well known results for the classical Ising model. In section IV we include the effect of correlations in the Quantum Ising model and discuss its properties.

I. METHOD

The hierarchy of correlations can be easily implemented in terms of double-time Green's functions, however, the particular exchange properties of spins may lead to many different descriptions (one can use a mapping to bosonic, fermionic or hardcore boson models). Here we consider a description in terms of fermionic Green's functions to avoid the $\omega = 0$ pole problem¹⁹, in combination with the Majorana representation for spins^{22,23}. This allows to directly work with fermionic Green's functions and operators, unifying the formalism and simplifying some of the calculations. The Majorana representation of a spin \vec{S}_n at site n is given by:

$$S_n^\alpha = -\frac{i}{2}\epsilon_{\alpha\beta\gamma}\eta_n^\beta\eta_n^\gamma \quad (1)$$

where η_n^α corresponds to a Majorana particle at site n with internal degree of freedom $\alpha = x, y, z$, and $\epsilon_{\alpha\beta\gamma}$ is the Levi-Civita symbol. The algebra of Majorana particles is characterized by $\{\eta_n^\alpha, \eta_m^\beta\} = \delta_{\alpha,\beta}\delta_{n,m}$, $(\eta_n^\beta)^2 = \frac{1}{2}$, $(\eta_n^\beta)^\dagger = \eta_n^\beta$ and one advantage is that it reproduces the $SU(2)$ algebra, preserving the rotational symmetry (which does not happen with e.g., the hard-core boson representation). As an example, the magnetization along the z-axis simply corresponds to $\langle S_n^z \rangle = -i\langle \eta_n^x \eta_n^y \rangle$. Note that another advantage of this representation is that it is local, which makes simple the interpretation of the results in the original language of spins.

To set up the hierarchy of correlations in position space one needs to find the scaling properties of spatial correlations between spins. For this we shall follow a previous derivation based on the monogamy property of entanglement²¹. Consider the Ising model in a transverse field Hamiltonian:

$$H = -B \sum_i S_i^x - \sum_{i,j>i} V_{i,j} S_i^z S_j^z \quad (2)$$

where the first term corresponds to the coupling to a transverse magnetic field B , and $V_{i,j}$ corresponds to the spin-spin interaction (because the mapping to Majorana fermions is local, this discussion can be done in the spin or Majorana fermion language). The large anisotropy in the spin-spin interaction, is usually present in real experiments due to the crystal field magnetization. Applying the Majorana representation we obtain the next Hamiltonian:

$$H = iB \sum_i \eta_i^y \eta_i^z + \sum_{i,j>i} V_{i,j} \eta_i^x \eta_i^y \eta_j^x \eta_j^y \quad (3)$$

For the study physical properties of the system we define the next double-time Green's function:

$$G_{n,m}^{\alpha,\beta}(t,t') = -i\langle \eta_n^\alpha(t); \eta_m^\beta(t') \rangle \quad (4)$$

where $\langle \dots \rangle$ corresponds to the statistical average with respect to a thermal density matrix $\hat{\rho} = e^{-\beta\hat{H}}$ at temperature $T = \beta^{-1}$, and ; indicates that we can use either the

time ordered, retarded or advanced Green's function, as they all fulfill the same equation of motion. The temperature is usually related with the Boltzmann distribution of a Markovian phonon bath that is in equilibrium with the system via spin-phonon coupling, which for simplicity we do not include in our description. We calculate the Green's function from the Heisenberg equation of motion $i\partial_t \mathcal{O} = [H, \mathcal{O}]$, which after a Fourier transformation to frequency domain reads:

$$\omega G_{n,m}^{\alpha,\beta}(\omega) = \frac{\delta_{n,m}}{2\pi} \delta_{\alpha,\beta} + iB\epsilon_{x\alpha\theta} G_{n,m}^{\theta,\beta}(\omega) + \epsilon_{z\alpha\theta} \sum_{i \neq n} V_{n,i} G_{i,n}^{xy\theta,\beta}(\omega) \quad (5)$$

where $G_{i,n}^{xy\mu,\beta}(t,t') = -i\langle \eta_i^x(t) \eta_i^y(t) \eta_n^\mu(t); \eta_n^\beta(t') \rangle$. Eq.5 is the central object of this work, as the Majorana double-time Green's function characterizes the order parameter $\langle S_n^z \rangle$, and differentiates between the FM and the PM phase. To find the scaling properties of correlations and obtain a decoupling scheme for higher correlation functions let us consider the diagonal part of the Green's function ($n = m$), which is related with the on-site magnetization. The four-point function $G_{i,n}^{xy\alpha,\beta}$, proportional to the reduced density matrix $\rho_{i,n}$, can then be separated into its uncorrelated and correlated parts according to the general decomposition $\rho_{i,n} = \rho_i \rho_n + \rho_{i,n}^C$. This allows to rewrite the equation of motion as:

$$\omega G_{n,n}^{\alpha,\beta}(\omega) = \frac{\delta_{\alpha,\beta}}{2\pi} + iB\epsilon_{x\alpha\theta} G_{n,n}^{\theta,\beta}(\omega) + \epsilon_{z\alpha\theta} \sum_{i \neq n} V_{n,i} \langle \eta_i^x \eta_i^y \rangle G_{n,n}^{\theta,\beta}(\omega) + \epsilon_{z\alpha\theta} \sum_{i \neq n} V_{n,i} \mathcal{G}_{i,n}^{xy\theta,\beta}(\omega) \quad (6)$$

where $G_{n,n}^{\alpha,\beta} \propto \rho_n$ and $\mathcal{G}_{i,n}^{\alpha\delta\gamma,\beta} \propto \rho_{n,i}^C$ correspond to the uncorrelated and correlated parts, respectively. If the system is strongly correlated, the entanglement monogamy implies that there is an upper bound to the amount of entanglement that a set of spins can share, i.e. we cannot correlate the set with an extra spin unless the entanglement in the initial set is reduced. In a system with dominant nearest neighbors interaction, one would expect that each spin is mainly entangled with its nearest neighbors; then if we have to reduce the entanglement between them to include an extra spin, it must decrease as $\rho_{i,n}^C \sim \mathcal{Z}^{-1}$; otherwise we would violate the entanglement monogamy. Finally, it can be shown that the scaling $\rho_{i,n}^C \sim \mathcal{Z}^{-1}$ implies $V_{i,j} \sim \mathcal{Z}^{-1}$ by calculating the equation of motion for the reduced density matrix. The meaning of the \mathcal{Z}^{-1} scaling is that contributions due to entanglement between spins must scale inversely with the coordination number. Finally, once we have fixed the scaling properties of correlations $\rho_{i,n}^C \sim \mathcal{Z}^{-1}$ and $V_{i,j} \sim \mathcal{Z}^{-1}$, we can organize the different terms in the equation of motion hierarchically and find their solution. It is important to stress that the assumption of a strongly correlated phase allows to derive

an upper bound to the scaling of correlations; however, if the phase is weakly correlated, one would expect an even smaller contribution from the correlated part.

To conclude this section, we discuss some general properties of the quantum Ising model in equilibrium at $T = 0$, which can be used to check our results: (i) the transverse magnetization $\langle S_i^y \rangle = 0$ to all orders of correlations, which can be proved from the calculation of the equation of motion $\partial_t \langle S_i^z \rangle = 0$; (ii) the two-point correlation function $\langle S_i^z S_j^y \rangle = 0$ to all orders, according to the equation of motion $\partial_t \langle S_i^x \rangle = 0$. Also, let us include the Fourier transform to \mathbf{k} -space of Eq.6, which will be used in the last sections:

$$\begin{aligned} \omega G_{\mathbf{k}}^{\alpha,\beta}(\omega) &= N \frac{\delta(\mathbf{k}) \delta_{\alpha,\beta}}{2\pi} + iB\epsilon_{x\alpha\theta} G_{\mathbf{k}}^{\theta,\beta}(\omega) \quad (7) \\ &+ \epsilon_{z\alpha\theta} \frac{1}{N} \sum_{\mathbf{q}} V_{\mathbf{q}} \langle \eta_{\mathbf{q}}^x \eta_{\mathbf{q}}^y \rangle G_{\mathbf{k}-\mathbf{q}}^{\theta,\beta}(\omega) \\ &+ \epsilon_{z\alpha\theta} \frac{1}{N} \sum_{\mathbf{q}} V_{\mathbf{q}} \mathcal{G}_{\mathbf{q},\mathbf{k}-\mathbf{q}}^{xy\theta,\beta}(\omega) \end{aligned}$$

In the next section we will show that one can simplify the second line, by assuming spatially homogeneous magnetization $\langle \eta_{\mathbf{q}}^x \eta_{\mathbf{q}}^y \rangle = \langle \eta^x \eta^y \rangle iN \delta(\mathbf{q}) = iM_z N \delta(\mathbf{q})$ (this choice is discussed in the next section, but should hold for ferromagnetic interaction and periodic boundary conditions).

II. UNCORRELATED SOLUTION

To characterize the ground state properties we are interested in the magnetization $\langle S_n^z \rangle$, which is related with the Majorana Green's function $G_{n,n}^{y,x}(t,t')$. If we neglect all terms proportional to \mathcal{Z}^{-1} , we find that the equation of motion, to lowest order, reduces to:

$$\begin{aligned} \omega \bar{G}_{n,n}^{\alpha,\beta} &= \frac{\delta_{\alpha,\beta}}{2\pi} + i\epsilon_{x\alpha\theta} B \bar{G}_{n,n}^{\theta,\beta} \quad (8) \\ &+ \epsilon_{z\alpha\theta} \sum_{i \neq n} V_{n,i} \langle \eta_i^x \eta_i^y \rangle \bar{G}_{n,n}^{\theta,\beta} \end{aligned}$$

where the bar on $\bar{G}_{n,n}^{\alpha,\beta}$ indicates the lowest order contribution to the Green's function $G_{n,n}^{\alpha,\beta}$, in powers of $1/\mathcal{Z}$. Note that the \mathcal{Z}^{-1} scaling coming from $V_{n,i}$ gets compensated by the sum over \mathcal{Z} neighbors, and all terms in the equation are of order one. The solution is easily found to be:

$$\bar{G}_{n,n}^{y,x} = -\frac{\sum_{i \neq n} V_{n,i} \langle \eta_i^x \eta_i^y \rangle}{2\pi(\omega^2 - \omega_n^2)} \quad (9)$$

where the poles of the Green's function are at $\pm\omega_n = \pm\sqrt{B^2 - \left(\sum_{i \neq n} V_{n,i} \langle \eta_i^x \eta_i^y \rangle\right)^2}$. Then the finite temperature, on-site magnetization, can be obtained from the

equal-time correlator¹⁷:

$$\begin{aligned} \langle \eta_n^x \eta_n^y \rangle &= i \int \frac{\bar{G}_{n,n}^{y,x}(\omega + i\epsilon) - \bar{G}_{n,n}^{y,x}(\omega - i\epsilon)}{e^{\beta\omega} + 1} d\omega \\ &= \frac{\sum_{i \neq n} V_{n,i} \langle \eta_i^x \eta_i^y \rangle}{2\omega_n} \tanh\left(\frac{\omega_n}{2T}\right) \quad (10) \end{aligned}$$

Clearly this is a complicated self-consistency equation, as the magnetization at site n couples to the magnetization at the sites connected by $V_{n,i}$. Hence, the solution clearly depends on the boundary condition and on the details of the interaction. Assuming periodic boundary conditions and ferromagnetic interaction, one can see that the solution that minimizes the average energy $\langle H \rangle$ corresponds to homogeneous magnetization. Hence, we drop the sub-index n and rewrite the equation in terms of the uncorrelated, average magnetization $\bar{M}_z = -i \sum_n \langle \eta_n^x \eta_n^y \rangle / N$:

$$\bar{M}_z = \frac{\bar{M}_z V_0}{2\omega_0} \tanh\left(\frac{\omega_0}{2T}\right) \quad (11)$$

where $\omega_0 = \sqrt{B^2 + V_0^2 \bar{M}_z^2}$ and $V_{\mathbf{k}} = \sum_{\mathbf{x}} e^{i\mathbf{k}\cdot\mathbf{x}} V_{\mathbf{x}}$. Similarly, the calculation of the transverse magnetization results in

$$\bar{M}_x = \frac{B}{2\omega_0} \tanh\left(\frac{\omega_0}{2T}\right) \quad (12)$$

$$\bar{M}_y = 0 \quad (13)$$

These equations reproduce the well know mean field self-consistency equations of the Ising model²⁴, and the phase diagram can be determined from their solution. We consider a 1D chain ($\mathcal{Z} = 2$), a square lattice ($\mathcal{Z} = 4$) and a cubic lattice ($\mathcal{Z} = 6$), and plot in Fig.1(solid line) the value of the magnetization as a function of the transverse field at $T = 0$. It shows that, for vanishing transverse field, all spins are aligned in parallel, minimizing the mean-field energy per spin $\langle H \rangle / N = -\bar{M}_z^2 V_0$. As the transverse field increases, quantum fluctuations $|\uparrow\rangle \leftrightarrow |\downarrow\rangle$ are produced, and for $B > V_0/2$ the longitudinal magnetization vanishes. This is the hallmark of the paramagnetic/ferromagnetic transition. Fig.2(solid line) corresponds to the finite-temperature phase diagram for the FM/PM phase transition, where now the temperature produces thermal fluctuations, destroying the ferromagnetic phase at the Curie temperature T_c .

From the uncorrelated results one finds the critical points expected from the mean field solution of the Ising model: $B_c(T = 0) = V_0/2$ and $T_c(B = 0) = V_0/4$, where $\mathcal{Z}V = V_0$. Note that in absence of correlations, the lattice dimension does not affect the result (just \mathcal{Z} is present), which usually leads to violations of the no-go theorems for quantum phase transitions in 1D and 2D^{25,26}. For example, this happens in the 1D classical Ising model ($B = 0$ in the present Hamiltonian), where it is known that the ferromagnetic phase is destroyed by thermal fluctuations. We will see in the next section that the addition of interspin correlations in the equation of motion allows to capture this feature. For the 1D Quantum

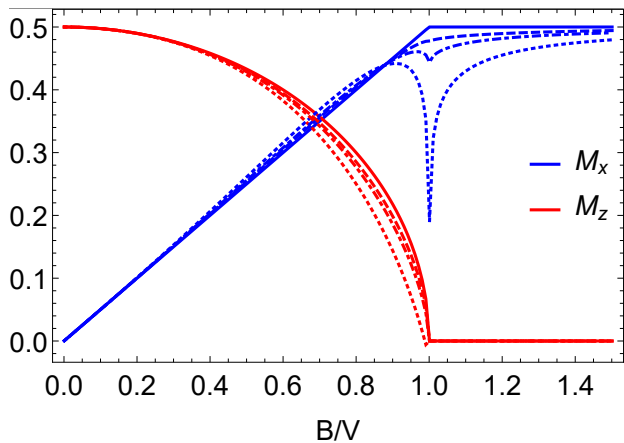


Figure 1: The solid lines correspond to the uncorrelated magnetization, as a function of the transverse field B/V for $T = 0$, where we have re-scaled the field to $B \rightarrow B/D$ to match the critical point in different dimensions. In dotted, dot-dashed and dashed we plot the magnetization including correlations to lowest order, as a function of external field, for $D = 1, 2$ and 3 , respectively. The correlated solution in 1D shows large deviations from \bar{M}_x around the critical point $B \lesssim B_c$ due to large correlations, however, they are reduced as D increases. Importantly, the critical point characterized by M_z is unchanged by correlations, in agreement with the exact solution of the transverse Ising model in 1D.

In the Ising model one can exactly solve the equations using the Wigner-Jordan transformation, and this allows us to compare our results with the exact solution. In this case, the $T = 0$ critical point is already reproduced by the uncorrelated solution, although the quasi-particle spectrum and critical properties are not²⁷.

It is worth to stress that we have highly simplified the mean field solution by assuming ferromagnetic interaction and periodic boundary conditions in Eq.10. In general, the mean field solution can be very powerful and it would capture interesting effects, as for example the dimerization induced by anti-ferromagnetic interaction, or frustration for some specific boundary conditions.

Critical properties in absence of correlations: It is known that near a quantum critical point, the system's properties can be characterized solely by its critical exponents²⁸ and that this feature leads to the important concept of universality classes. Here we discuss some of the critical properties of the hierarchy in absence of correlations. Although all mean field theories are characterized by the same critical exponents, independently of the system's dimension, we will first show how one can obtain their value from the previous results, and then in the next sections, compare with the case when interspin correlations are included.

In absence of correlations, we can use the self-consistency equation (Eq.11) to calculate the critical exponent β near T_c and B_c : In the FM phase and near the critical temperature we have $t, \bar{M}_z \ll 1$, where $t = (T_c - T)/T_c$ is the reduced temperature. Then the

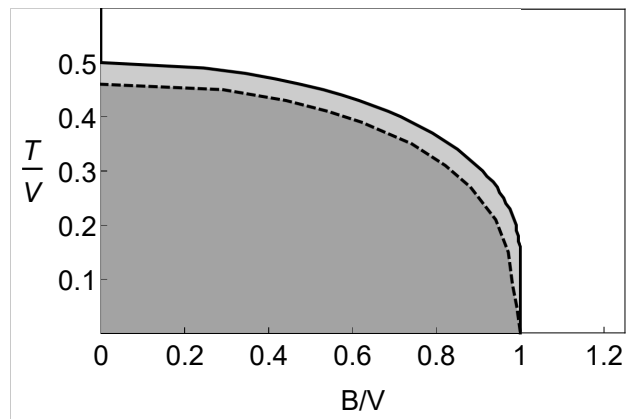


Figure 2: The solid (dashed) line corresponds to the uncorrelated (correlated to lowest order) phase diagram as a function of the transverse field B/V and temperature T/V for a spin chain in arbitrary dimension (we re-scale $T \rightarrow T/D$ and $V \rightarrow V/D$ to make the critical lines coincide in absence of correlations). Shaded area corresponds to the ferromagnetic phase. We have omitted the phase diagram including correlations for the 2D and the 3D case, as they are almost coincident with the mean field result. This is in agreement with the decreasing role of correlations in higher dimensions.

magnetization can be approximated as ($B = 0$):

$$\bar{M}_z = \frac{1}{2} \tanh\left(\frac{2\bar{M}_z}{1-t}\right) \simeq \frac{\bar{M}_z}{1-t} - \frac{1}{6} \left(\frac{2\bar{M}_z}{1-t}\right)^3 + \mathcal{O}(\bar{M}_z^5) \quad (14)$$

where we have used the series expansion $\tanh(x) \simeq x - \frac{x^3}{3} + \mathcal{O}(x^5)$. The solutions to lowest order in t are:

$$\bar{M}_z = 0, \quad \bar{M}_z = \pm \frac{\sqrt{3t}}{2} \quad (15)$$

which imply that the critical exponent for the order parameter near T_c is $\beta_t = 1/2$. If in a similar manner we analyze the critical behavior near B_c , as a function of the reduced field $b = (B_c - B)/B_c$. We find:

$$\bar{M}_z^2 = \frac{b}{2} - \frac{b^2}{4} \simeq \frac{b}{2} \quad (16)$$

and the solutions for the magnetization are:

$$\bar{M}_z = 0, \quad \bar{M}_z = \pm \sqrt{\frac{b}{2}} \quad (17)$$

with the corresponding critical exponent $\beta_b = 1/2$. Note that we differentiate the critical exponent near B_c and T_c because the first corresponds to a quantum critical point, while the second to a classical one. As expected for mean field solutions, both relevant parameters have identical critical exponents $\beta = 1/2$. The anomalous dimension η and the correlation length ξ must be obtained from the correlated part of the two-point function $\langle S_{\mathbf{k}}^z S_{\mathbf{k}'}^z \rangle_C$, which vanishes at this order of the hierarchy – This is in contrast with some refined calculations of the mean

field solution, where the fluctuation-dissipation theorem is used, giving a non-vanishing correlated part²⁹. Equivalently, corresponds to the difference between Landau and Ginzburg–Landau theory. We will show in the next section that this is captured adding first order perturbations to the uncorrelated solution.

III. CORRELATIONS IN ABSENCE OF TRANSVERSE FIELD

Now we consider the next order in the hierarchy of correlations, and include $\mathcal{O}(\mathcal{Z}^{-1})$ terms. We expect that the corrections due to correlations will become more important as we approach the phase boundary, as it is known that at the phase boundary, the system becomes critical and interspin correlations diverge. Furthermore, as \mathcal{Z} changes with the dimension, we would expect that the scaling of corrections due to correlations is worse in the 1D case, while 2D and 3D should display smaller contributions.

Now the term $\mathcal{G}_{iin,n}^{xy\mu,\beta}$ that was neglected in absence of correlations in Eq.6 contributes and must be included. We calculate the equation of motion for the correlated part of the four-point function $G_{ppn,n}^{xy\alpha,\beta} = -i\langle\eta_p^x\eta_p^y\eta_n^\alpha;\eta_n^\beta\rangle$ in the Appendix. This is done by calculating the equation of motion for the four-point function, removing the uncorrelated part $\langle\eta_p^x\eta_p^y\rangle G_{n,n}^{\alpha,\beta}$, and neglecting terms of $\mathcal{O}(\mathcal{Z}^{-2})$ or higher. The solution for the four-point function, including the transverse field, can be obtained analytically, however it is too long to be explicitly written here. For simplicity let us first consider the model in absence of a transverse field ($B = 0$). In this case the solution for the correlated part highly simplifies, and one finds that the Fourier transform of $\mathcal{G}_{iin,n}^{xy\mu,\beta}$ is:

$$\mathcal{G}_{\mathbf{k},\mathbf{k}'}^{xy\alpha,\beta} = -\frac{\omega\Lambda_{\mathbf{k},\mathbf{k}'}^{\alpha,\beta} + \epsilon_{z\alpha\theta}iV_0M_z\Lambda_{\mathbf{k},\mathbf{k}'}^{\theta,\beta}}{\omega^2 - V_0^2M_z^2} \quad (18)$$

where

$$\Lambda_{\mathbf{k},\mathbf{k}'}^{\alpha,\beta} = \epsilon_{z\alpha\theta} \left(\frac{1}{4} - M_z^2 \right) V_{-\mathbf{k}} G_{\mathbf{k}+\mathbf{k}'}^{\theta,\beta} - \frac{\epsilon_{z\alpha\theta}}{N} \sum_{\mathbf{q}} V_{\mathbf{q}} \langle \eta_{\mathbf{k}}^x \eta_{\mathbf{k}}^y \eta_{\mathbf{q}}^x \eta_{\mathbf{q}}^y \rangle_C G_{\mathbf{k}'-\mathbf{q}}^{\theta,\beta} \quad (19)$$

At this point, the simplest approximation that one can make is to substitute the Green's functions $G_{\mathbf{k}}^{\theta,\beta}$ in $\Lambda_{\mathbf{k},\mathbf{k}'}^{\alpha,\beta}$, by its uncorrelated solution $\bar{G}_{\mathbf{k}}^{\theta,\beta}$. Then one can solve the self-consistency equation for the equal-time correlator $\langle \eta_{\mathbf{k}}^x \eta_{\mathbf{k}}^y \eta_{\mathbf{k}'}^x \eta_{\mathbf{k}'}^y \rangle_C$ and find:

$$\begin{aligned} \langle S_{\mathbf{k}}^z S_{\mathbf{k}'}^z \rangle_C &= -\langle \eta_{\mathbf{k}}^x \eta_{\mathbf{k}}^y \eta_{\mathbf{k}'}^x \eta_{\mathbf{k}'}^y \rangle_C \\ &= \frac{N\delta_{\mathbf{k},-\mathbf{k}'} V_{\mathbf{k}'} \left(\frac{1}{4} - \bar{M}_z^2 \right)}{4T \cosh^2 \left(\frac{V_0 \bar{M}_z}{2T} \right) - V_{\mathbf{k}'}} \end{aligned} \quad (20)$$

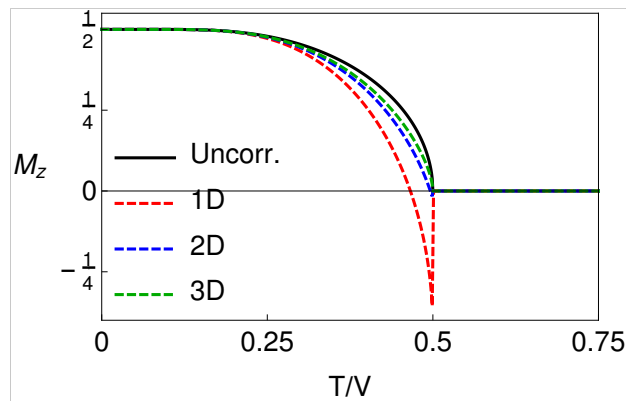


Figure 3: Numerical calculation of the average magnetization including lowest order correlations, as a function of T for $D = 1, 2, 3$ (red, blue and green, respectively). In $D = 1$ we obtain an unphysical remnant magnetization, which is cured by including feedback (Fig.4). For $D \geq 2$ the discontinuity is washed out and the corrections smaller. The critical point has been re-scaled to $T_c \rightarrow T_c/D$, to make it coincident for all cases.

As expected in absence of the transverse field (i.e., quantum fluctuations), the correlation function $\langle S_{\mathbf{k}}^z S_{\mathbf{k}'}^z \rangle_C$ vanishes. On the other hand, longitudinal correlations $\langle S_{\mathbf{k}}^z S_{\mathbf{k}'}^z \rangle_C$ vanish at $T = 0$, where the exact \mathbf{Z}_2 ground state of the system is given by a product state of polarized spins along z , as well as for $T \rightarrow \infty$, where the ground state corresponds to an incoherent set of decoupled spins. The transition mechanism between the two limits corresponds to a competition between thermal fluctuations and spin-spin interactions. It is interesting the appearance of a mass term in Eq.20 due to the solution of the self-consistency equation, which is proportional to $T - T_c$ (just by expanding $V_{\mathbf{k}}$ in powers of \mathbf{k} and setting $V_0 = 4T_c$); this is very similar to the mass term obtained in ϕ^4 -theory when the Hubbard-Stratonovich transformation is applied to the Ising model.

From Eq.7 it is clear that the magnetization will now include corrections due to interspin correlations. Inserting Eq.20 into Eq.7 we find:

$$M_z = \bar{M}_z - \left(\frac{1}{4} - \bar{M}_z^2 \right) \frac{1}{N} \sum_{\mathbf{q}} \frac{\frac{|V_{\mathbf{q}}|^2}{2T} \tanh \left(\frac{V_0 \bar{M}_z}{2T} \right)}{4T \cosh^2 \left(\frac{V_0 \bar{M}_z}{2T} \right) - V_{\mathbf{q}}} \quad (21)$$

where \bar{M}_z is the average magnetization, previously obtained in absence of correlations. The sign of the correction term shows that interspin correlations mostly act against the formation of ferromagnetic order, and as in 1D these corrections will be larger, we expect that the FM phase should be significantly reduced. Its numerical calculation for different dimensions is shown in Fig.3 (the divergence due to a vanishing denominator in Eq.21 is automatically cured by the input of the mean field values \bar{M}_z). It shows that due to thermal fluctuations, the ferromagnetic phase shrinks down for all cases, and in 1D

it changes sign close to T_c . This result is unphysical and it is produced due to the poor scaling of correlations in 1D, where $Z = 2$. As we approach the critical point, correlations between spins increase, and contributions from Z^{-n} terms, with $n > 2$, become important. The fact that in 1D we observe a stronger influence of correlations is also related with the fact that the ferromagnetic phase in 1D should be destroyed by the thermal fluctuations at arbitrary $T \neq 0$ and the two main sources of this failure are: (1) The use of the uncorrelated Green's functions in Eq.18, neglecting the feedback of the magnetization in the interspin correlations, and (2) higher n-point functions will become increasingly dominant according to renormalization group arguments. The first issue can be easily fixed by rewriting the equation of motion as a Dyson's equation, as we show next. The implementation of a renormalization group analysis will be performed in future publications.

To include back-reaction between the renormalized magnetization and the interspin correlations we insert Eq.18 into Eq.7. As the magnetization is spatially homogeneous the equation of motion can be written as:

$$\omega G_0^{\alpha,\beta} = \frac{\delta_{\alpha,\beta}}{2\pi} + \epsilon_{z\alpha\theta} i M_z V_0 G_0^{\theta,\beta} + \chi \frac{\omega G_0^{\alpha,\beta} + \epsilon_{z\alpha\theta} i V_0 M_z G_0^{\theta,\beta}}{\omega^2 - V_0^2 M_z^2} \quad (22)$$

where we have defined

$$\chi = \frac{1}{N} \sum_{\mathbf{q}} |V_{\mathbf{q}}|^2 \left[\frac{1}{4} - M_z^2 - \frac{1}{N} \langle \eta_{\mathbf{q}}^x \eta_{\mathbf{q}}^y \eta_{-\mathbf{q}}^x \eta_{-\mathbf{q}}^y \rangle_C \right] \quad (23)$$

and $G_0^{\alpha,\beta} = G_{\mathbf{k}=0}^{\alpha,\beta}/N$. This can be written in matrix form as follows:

$$\omega \hat{G} = \frac{\hat{\delta}}{2\pi} + \hat{H}_0 \cdot \hat{G} + \hat{\Sigma}(\omega) \cdot \hat{G} \quad (24)$$

and if we define the uncorrelated Green's function matrix as $\hat{G}^{(0)} = [\omega - \hat{H}_0]^{-1}$, we find the usual Dyson's like equation:

$$\hat{G} = \hat{G}^{(0)} \cdot \frac{\hat{\delta}}{2\pi} + \hat{G}^{(0)} \cdot \hat{\Sigma}(\omega) \cdot \hat{G} \quad (25)$$

with frequency dependent self-energy

$$\hat{\Sigma}(\omega) = \chi \frac{\hat{\sigma}_0 \omega - \hat{\sigma}_y V_0 M_z}{\omega^2 - V_0^2 M_z^2} \quad (26)$$

being $\hat{\delta} = (\delta_{x,\beta}, \delta_{y,\beta})^T$, $\sigma_y = \begin{pmatrix} 0 & -i \\ i & 0 \end{pmatrix}$ and $\hat{\sigma}_0$ the identity matrix. The solution for the Green's function can be obtained by direct matrix inversion:

$$\hat{G} = \left[\omega - \hat{H}_0 - \hat{\Sigma}(\omega) \right]^{-1} \cdot \frac{\hat{\delta}}{2\pi} \quad (27)$$

We can now compare the full solution (Eq.27) with the one obtained in Eq.21. It is equivalent to the substitution

of \hat{G} by $\hat{G}^{(0)}$ on the rhs of Eq.24, and then equivalent to first order perturbation over the mean field value. This explains the breakdown for the magnetization as one approaches the phase boundary in Fig.3.

In Eq.27 back-reaction between G and \mathcal{G} is now included, and although the formal solution seems simple, the calculation of the self-energy can be quite complicated. The reason is that it contains terms proportional to $\langle \eta_{\mathbf{q}}^x \eta_{\mathbf{q}}^y \eta_{-\mathbf{q}}^x \eta_{-\mathbf{q}}^y \rangle_C$, which must be determined self-consistently with M_z . As the purpose of this manuscript is to discuss the application of the hierarchy of correlations to general spins systems, and not to fully characterize the Ising model (for which a large number of accurate results is already available), we will only analyze the full solution for the 1D case, proving that the suppression of the ferromagnetic phase is captured in very simple terms. Results in higher dimensions should be even more accurate, which shows the power of this approach.

As we will discuss below for the general case, one of the advantages of the Ising model with $B = 0$ is that the frequency dependence of the self-energy can be pulled out of the integral over \mathbf{q} . This allows to exactly calculate the poles of the Green's function when interspin correlations are included. In the presence of correlations, the poles obtained in absence of correlations separate in pairs, and their splitting is proportional to the strength of correlations $\omega = \pm V_0 M_z \pm \sqrt{\chi}$. We expect that the addition of higher spin correlations will induce new poles as well, approaching a continuum in the real axis, as it is expected in the thermodynamic limit.

Before we fully solve the self-consistency equation, let us consider a slightly easier calculation, which also provides some insight into the effect of correlations in the Ising model. This consists in approximating the statistical average in the self-energy $\langle \eta_{\mathbf{q}}^x \eta_{\mathbf{q}}^y \eta_{-\mathbf{q}}^x \eta_{-\mathbf{q}}^y \rangle_C$ by its lowest order expression (Eq.20):

$$\chi = \left(\frac{1}{4} - M_z^2 \right) \frac{1}{N} \sum_{\mathbf{q}} \frac{4T \cosh^2 \left(\frac{V_0 M_z}{2T} \right) |V_{\mathbf{q}}|^2}{4T \cosh^2 \left(\frac{V_0 M_z}{2T} \right) - V_{-\mathbf{q}}} \quad (28)$$

In this case one neglects the self-consistency equation for $\langle \eta_{\mathbf{q}}^x \eta_{\mathbf{q}}^y \eta_{-\mathbf{q}}^x \eta_{-\mathbf{q}}^y \rangle_C$ and just M_z is determined self-consistently. This solution corresponds to what one would expect from the Random Phase Approximation (RPA). The explicit calculation of Eq.28 diverges when $4T \cosh^2 \left(\frac{V_0 M_z}{2T} \right) < V_0$; this is an instability inherent to the RPA calculation, indicating that the ground state is unstable with respect to these collective excitations³⁰ (because thermal excitations will shift the phase boundary or even destroy the ferromagnetic phase). Generally the divergence is corrected by the addition of the collective mode contributions to the self-energy, and in our case, it will be cured by including the self-consistency equation for $\langle \eta_{\mathbf{q}}^x \eta_{\mathbf{q}}^y \eta_{-\mathbf{q}}^x \eta_{-\mathbf{q}}^y \rangle_C$, instead of using its lowest order approximation.

Now to obtain the full solution we calculate M_z from the Green's function in Eq.27, and χ from Eq.18 with $G_0^{\alpha,\beta}$ from Eq.27. After some simple manipulations one

finds:

$$M_z = \frac{\frac{1}{2} \sinh\left(\frac{V_0 M_z}{T}\right)}{\cosh\left(\frac{V_0 M_z}{T}\right) + \cosh\left(\frac{\sqrt{\chi}}{T}\right)} \quad (29)$$

$$\chi = \left(\frac{1}{4} - M_z^2\right) \frac{1}{N} \sum_{\mathbf{q}} \frac{m |V_{\mathbf{q}}|^2}{m - \frac{V_{\mathbf{q}}}{V_0}} \quad (30)$$

with $m = 2\sqrt{\chi} \left[\cosh\left(\frac{M_z V_0}{T}\right) + \cosh\left(\frac{\sqrt{\chi}}{T}\right) \right] / V_0 \sinh\left(\frac{\sqrt{\chi}}{T}\right)$. Eqs.29 and 30 are one of the main results. They correspond to the generalization of the mean field equation for the magnetization, now including the effect of interspin correlations. They are valid in arbitrary dimension, and both reduce to the mean field case if $\chi \rightarrow 0$. It is important to note that Eq.30 has a divergence, however its different to the RPA one previously obtained, and basically restricts χ to positive values. This is physically meaningful because χ corresponds to the integral of $\langle S_{\mathbf{k}}^z S_{-\mathbf{k}}^z \rangle_C$ over the whole Brillouin zone, which is always positive because they tend to be aligned. The positivity of χ also makes the poles of the Green's function to be real valued. Finally, we also include the calculation of the average energy per spin (details of the calculation in the Appendix):

$$E_0 = -V_0 M_z^2 - \frac{\frac{1}{2} \sqrt{\chi} \sinh\left(\frac{\sqrt{\chi}}{T}\right)}{\cosh\left(\frac{V_0 M_z}{T}\right) + \cosh\left(\frac{\sqrt{\chi}}{T}\right)} \quad (31)$$

The second term shows that interspin correlations always reduce the energy and stabilize the system. Now we particularize the previous expressions to 1D and study the fate of the ferromagnetic phase when correlations are included. The self-consistency equation in the continuum limit for χ (Eq.30) can be calculated analytically by contour integration in the complex plane, leading to ($V_{\mathbf{q}} = V_0 \cos(q)$):

$$\chi_{1D} = \frac{\left(\frac{1}{4} - M_z^2\right) m^2 V_0^2}{m^2 - 1 + m\sqrt{m^2 - 1}} \quad (32)$$

Fig.4 shows the solution to the self-consistency equations Eq.29 and Eq.30. We find that the phase with $M_z = 0$ is the one that persists in the presence of correlations, to arbitrary low temperature. We also plot the ground state energy as a function of temperature, and it shows that as the temperature decreases, interspin correlations increase and the energy of the paramagnetic ground state is reduced. Interestingly the self-consistency equations also have a solution corresponding to a first order transition for $T \sim 0.25V$, but its energy is higher than the one for $M_z = 0$.

These solutions to the self-consistency equations fully characterize the Green's functions in 1D. Higher dimensional cases can be solved in a similar way, with the difference that one does not have an analytical expression for the integral in Eq.30 and numerical methods must be used. Note that the addition of a longitudinal field

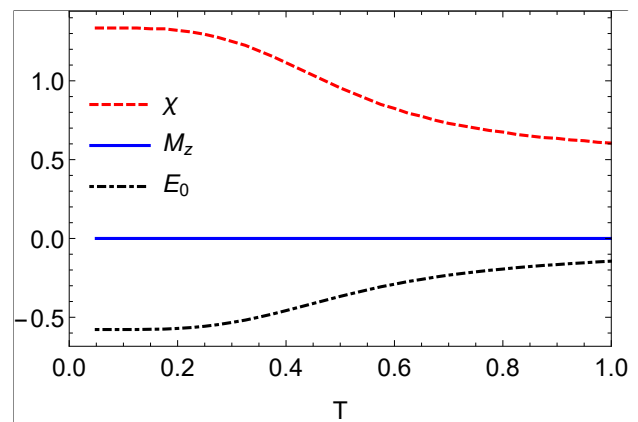


Figure 4: Full solutions to the self-consistency equations and average energy as a function of T/V for the 1D classical Ising model.

B_z is straightforward, and this calculation can easily be generalized.

Critical exponents: Finally, we analyze the effect of correlations on the critical exponents. As the phase transition is absent in 1D, one must consider $D \geq 2$ to discuss the critical exponents. This is a straightforward numerical calculation which requires to solve the self-consistency equations Eq.30 and Eq.29. However it does not provide a clear picture of the effect of correlations, and for this reason, we will discuss the lowest order solutions only, which can be done analytically. To lowest order, we can consider Eq.20 to describe interspin correlations. In the long wavelength limit of this expression, the dominant contribution is:

$$\langle S_{\mathbf{k}}^z S_{-\mathbf{k}}^z \rangle_C \propto \frac{4T_c \left(\frac{1}{4} - \bar{M}_z^2\right)}{4T \cosh^2\left(2\bar{M}_z \frac{T_c}{T}\right) - 4T_c + V k^2} \quad (33)$$

where $k = |\mathbf{k}|$ and we have renamed $V_0 = 4T_c$. The Fourier transform of Eq.33 is proportional to $e^{-\frac{|x|}{\xi}}$, which corresponds to exponential decay with correlation length:

$$\xi(T) = \frac{1}{2} \sqrt{\frac{V}{T \cosh^2\left(2\bar{M}_z \frac{T_c}{T}\right) - T_c}} \quad (34)$$

In Fig.5 we plot the temperature dependence of the correlation length for the Ising model in different dimensions. In all cases we find a divergence at the critical temperature T_c , and a decrease in ξ as one moves away from the critical point. To estimate the critical behavior of ξ near T_c , we expand in powers of the reduced temperature t , and to lowest order we find:

$$\xi = \frac{1}{2} \sqrt{\frac{V}{T_c t}} \rightarrow \nu = 1/2 \quad (35)$$

This is the critical exponent of Ginzburg–Landau theory, which is expected because we assumed the lowest order correction in the self-energy, corresponding to

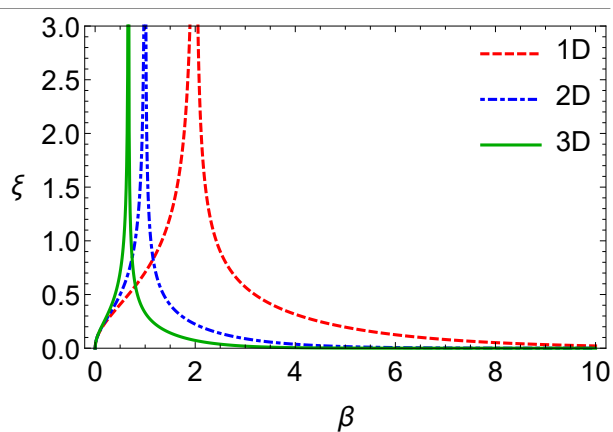


Figure 5: Correlation length $\xi(T)$ to lowest order in correlations, as a function of the inverse temperature β , in units of V . At the Curie temperature the correlation length diverges with critical exponent $\nu = 1/2$.

first order perturbation (Eq.20). Similarly, the anomalous dimension η can be obtained from the correlated part of the two-point function at $T = T_c$, which according to scaling arguments²⁹, must be proportional to $\langle S^z S^z \rangle_{k \ll 1}^C \propto k^{\eta-2}$. We find from Eq.33:

$$\langle S_k^z S_{-k}^z \rangle_C \propto k^{-2} \rightarrow \eta = 0 \quad (36)$$

meaning that the scaling of fields is not anomalous and agreeing with the expectations from Ginzburg–Landau theory. If we calculate the critical exponent β_t from Eq.21, we find $\beta_t = 1/2$. This critical exponent has not changed because we added correlations perturbatively, however the numerical calculation, including the feedback between the interspin correlations and the magnetization should display non-perturbative corrections. Nevertheless, in the next section we will show that even at this level, we can find some interesting differences between the quantum and the classical critical point.

IV. CORRELATIONS IN THE QUANTUM ISING MODEL

In this section we include the transverse field B and compare with the previous results. The solutions for the correlation functions $\mathcal{G}_{\mathbf{k}, \mathbf{k}'}^{xy\alpha, \beta}$ are obtained analytically, but their expressions are quite complicated. Hence we will discuss their general properties and then analyze in detail two different approximations: the perturbative solution over the whole phase diagram, and the non-perturbative solution within the paramagnetic phase. In this last case $B > B_c$ and $M_z = -i\langle \eta^x \eta^y \rangle = 0$, highly simplifying the expressions. Importantly, the $T = 0$ limit will allow us to compare the properties of the classical and quantum critical point.

In general, we find that due to the transverse field B , the correlation functions $\mathcal{G}_{\mathbf{k}, \mathbf{k}'}^{xy\alpha, \beta}$ display new collec-

tive excitations called magnons, with dispersion relationship $\hat{\omega}_{\mathbf{k}} = \sqrt{B^2 + V_0^2 M_z^2 - B M_x V_{\mathbf{k}}}$ (1D case shown in Fig.6). The dependence on the transverse magnetization M_x makes that, at the critical point $B_c = V_0/2$, the gap closes displaying linear dispersion around $\mathbf{k} \simeq 0$. This is related with the scale invariance of the system at low energies, when B is tuned to the critical value. As in the previous section we can write the corresponding Dyson's equation:

$$\omega \hat{G} = \frac{\hat{\delta}}{2\pi} + \hat{H}_0 \cdot \hat{G} + \hat{\Sigma} \cdot \hat{G} + \hat{\Sigma}_0 \quad (37)$$

where now $\hat{G} = (G_0^{x, \beta} \ G_0^{y, \beta} \ G_0^{z, \beta})^T$, $\hat{\delta} = (\delta_{x, \beta} \ \delta_{y, \beta} \ \delta_{z, \beta})^T$ and

$$\hat{H}_0 = i \begin{pmatrix} 0 & M_z V_0 & 0 \\ -M_z V_0 & 0 & B \\ 0 & -B & 0 \end{pmatrix} \quad (38)$$

The appearance of two different self-energy contributions $\hat{\Sigma}$ and $\hat{\Sigma}_0$ (homogeneous and inhomogeneous term, respectively) happens because the solutions to $\mathcal{G}_{\mathbf{q}, -\mathbf{q}}^{xy\alpha, \beta}$ contain terms proportional to $G_{n, n}^{\alpha, \beta}$ and $G_{nnn, n}^{xyz, \beta}$, respectively (actually the Green's function $G_{nnn, n}^{xyz, \beta}$ is closely related with the Φ field defined in ref.²²). Fortunately, $G_{nnn, n}^{xyz, \beta}$ can be calculated exactly from its equation of motion, and gives:

$$G_{nnn, n}^{xyz, \beta} = \frac{i}{2\pi\omega} (M_x \delta_{x, \beta} + M_y \delta_{y, \beta} + M_z \delta_{z, \beta}) \quad (39)$$

Therefore, $\hat{\Sigma}_0$ contributes to the source term $\hat{\delta}$, in addition to the previously discussed change in the quasiparticle pole coming from $\hat{\Sigma}$. The detailed form of the self-energies is complicated, and for practical purposes they must be manipulated numerically.

We first consider the lowest order solution by making the substitution $\hat{\Sigma} \cdot \hat{G} \rightarrow \hat{\Sigma} \cdot \hat{G}_0$ in Eq.37. In Fig.1 we plot the $T = 0$ magnetization vs the transverse field. As in the previous section, the corrections to the magnetization in absence of correlations are larger in low dimensions, however the corrections are smaller for the $T = 0$ line, and the magnetization in 1D does not drop to negative values close to the critical point. In Fig.2 we plot the full phase diagram, where one can see that thermal fluctuations affect more drastically to the phase diagram, specially as one approaches the classical critical point T_c . Interspin correlations at this order show that, within the ferromagnetic phase and for $B \neq 0$, the crossed correlation function $\langle S_{\mathbf{k}}^x S_{\mathbf{k}'}^z \rangle_C \neq 0$. This is what one would expect, as B introduces quantum fluctuations and $\bar{M}_{x, z}$ are both finite. In Fig.7 we plot the interspin correlation functions in 1D as the transverse magnetic field increases, crossing the critical point. It shows that correlations increase as one approaches the phase boundary, diverging for $\mathbf{k} = 0$ at the critical point. We do not show the 2D or 3D case in this plot, as the results are qualitatively the same (we

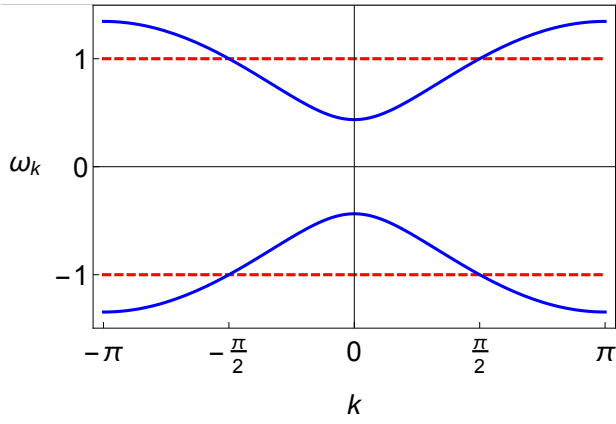


Figure 6: Poles of the Green's function vs \mathbf{k} obtained from the uncorrelated (dashed, red) and correlated (solid, blue) solution in 1D. We have chosen $B/V = 0.9$ and $Z = 2$ for the plot. At the critical point the gap closes.

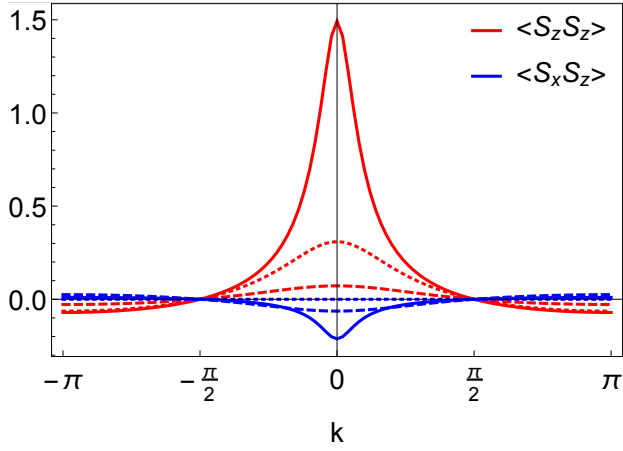


Figure 7: Correlated part of the spin-spin correlation functions $\langle S_{\mathbf{k}}^{\alpha} S_{-\mathbf{k}}^{\beta} \rangle$ vs \mathbf{k} in 1D (lowest order correction). We have chosen $T = 0$ and different values for the transverse field $B/V = 0.75, 0.99$ and 1.25 (dashed, solid and dotted, respectively). Correlations increase as we approach the critical point from both phases, and at the critical point, the system becomes scale invariant and correlations diverge at $\mathbf{k} = 0$.

find the same divergence at $\mathbf{k} = 0$ for $B = B_c$, and a slightly different behavior at large \mathbf{k}). The difference in sign between the longitudinal and the transverse correlations happens because the longitudinal try to align the spins parallel, while the transverse acts in opposition, trying to break the ferromagnetic order.

Finally, we consider the solution for the paramagnetic phase, by assuming $B > B_c$ and $M_z = 0$. This allows us to find compact analytical expressions and gain some insight into the main differences between the classical and the quantum Ising model. The first advantage of considering the paramagnetic phase is that the Green's function $G_0^{x,\beta}$ decouples from the rest, reducing the matrix dimension. The Dyson's equation is in this case:

$$\hat{G} = \frac{1}{2\pi} \hat{G}^{(0)} + \hat{G}^{(0)} \cdot \hat{\Sigma}(\omega) \cdot \hat{G} \quad (40)$$

where $\hat{G} = (G_0^{y,\beta} \ G_0^{z,\beta})^T$, $\hat{\Sigma}(\omega) = \lambda(\omega) \begin{pmatrix} 1 & 0 \\ 0 & 0 \end{pmatrix}$ and

$$\lambda(\omega) = \frac{\omega}{N} \sum_{\mathbf{q}} |V_{\mathbf{q}}|^2 \frac{\frac{1}{4} - \frac{1}{N} \langle \eta_{\mathbf{q}}^x \eta_{\mathbf{q}}^y \eta_{-\mathbf{q}}^x \eta_{-\mathbf{q}}^y \rangle_C}{\omega^2 - B^2 + M_x B V_{\mathbf{q}}} \quad (41)$$

One important difference between the self-energy in the previous section (Eq.26) and Eq.41 is that in this case, the non-commutativity of the interaction and transverse field terms in the Hamiltonian, mix the integral over \mathbf{q} and the ω dependence. Then the pole structure for the Green's function will depend on this integral and in consequence, on the properties of the interaction $V_{\mathbf{q}}$ and the dimension of the system. A full solution requires to determine $\langle S_{\mathbf{k}}^z S_{\mathbf{k}'}^z \rangle_C$ and solve self-consistently for the magnetization and $\lambda(\omega)$. This is why the full solution is significantly more complicated with the transverse field.

If we consider Eq.41, one can separate its real and complex parts $\lambda(\omega \pm i\eta) = \lambda_r(\omega) \mp i\lambda_i(\omega)$, being:

$$\lambda_r(\omega) = \text{PV} \frac{\omega}{N} \sum_{\mathbf{q}} |V_{\mathbf{q}}|^2 \frac{\frac{1}{4} + \frac{1}{N} \langle S_{\mathbf{q}}^z S_{-\mathbf{q}}^z \rangle_C}{2\sqrt{B^2 - B M_x V_{\mathbf{q}}}} \left(\frac{1}{\omega - \sqrt{B^2 - B M_x V_{\mathbf{q}}}} - \frac{1}{\omega + \sqrt{B^2 - B M_x V_{\mathbf{q}}}} \right) \quad (42)$$

$$\lambda_i(\omega) = \pi \frac{\omega}{N} \sum_{\mathbf{q}} |V_{\mathbf{q}}|^2 \frac{\frac{1}{4} + \frac{1}{N} \langle S_{\mathbf{q}}^z S_{-\mathbf{q}}^z \rangle_C}{2\sqrt{B^2 - B M_x V_{\mathbf{q}}}} \left[\delta\left(\omega - \sqrt{B^2 - B M_x V_{\mathbf{q}}}\right) - \delta\left(\omega + \sqrt{B^2 - B M_x V_{\mathbf{q}}}\right) \right] \quad (43)$$

where PV indicates the principal value. Then one can calculate the formal solution to Eq.40 by direct matrix

inversion:

$$G_0^{z,y}(\omega) = \frac{-iB}{2\pi [\omega^2 - B^2 - \omega\lambda(\omega)]} \quad (44)$$

which is a function of the self-energy. As the full solution requires to complement the Green's function with the self-consistency equation for M_x , we must obtain its corresponding spectral density:

$$\begin{aligned} J^{z,y}(\omega) &= i(e^{\beta\omega} + 1)^{-1} [G_0^{z,y}(\omega + i\eta) - G_0^{z,y}(\omega - i\eta)] \\ &= \frac{1}{\pi} \frac{-i(e^{\beta\omega} + 1)^{-1} B\gamma(\omega)}{[\omega^2 - B^2 - m(\omega)]^2 + \gamma(\omega)^2} \end{aligned} \quad (45)$$

where we have redefined the the complex and real parts in terms of the damping $\gamma(\omega) = \omega\lambda_i(\omega)$ and quasiparticle mass $m(\omega) = \omega\lambda_r(\omega)$, respectively. Then the self-consistency equation for M_x corresponds to:

$$iM_x = \int_{-\infty}^{\infty} J^{z,y}(\omega) d\omega \quad (46)$$

To fully characterize the self-energy in Eqs.42,43 one needs to obtain an expression for $\langle S_{\mathbf{q}}^z S_{-\mathbf{q}}^z \rangle_C$ from the solution of $\mathcal{G}_{\mathbf{q},-\mathbf{q}}^{xyx,y}$. An integral form of the solution is not very difficult to obtain, because the corresponding spectral density can be defined in terms of $G^{z,y}$ and the contributions from the poles at $\pm\sqrt{B^2 - BM_x V_{\mathbf{q}}}$. Then Eqs.42,43 and the self-consistency equation for M_x form a closed set of equations that fully characterize the paramagnetic phase. The solution needs to be obtained by numerical means, however one can see from Eq.45 that the two initial quasiparticle poles at $\omega = \pm B$ are now smeared out by interactions to a Lorentzian shape, and for $\gamma, m \rightarrow 0$ one recovers the uncorrelated self-consistency equation. The complex part of the self-energy γ produces damping and the real part m produces a shift in the quasiparticle energy. If the damping is small ($\gamma(\omega) \ll 1$) and the spectral function has maximums at $\omega = E_{\pm}$, with $m(\omega)$ and $\gamma(\omega)$ slow varying functions around them, we can define the quasiparticles dispersion by solving:

$$E_{\pm}^2 - B^2 - m(E_{\pm}) = 0 \quad (47)$$

This corresponds to approximate quasiparticles (magnons), slightly damped by interactions and with excitation energies E_{\pm} .

To estimate the effect of interactions in the paramagnetic phase, without solving the full self-consistency equations, we can proceed in a slightly simpler way if we insert the uncorrelated Green's function $\hat{G}^{(0)}$ on the rhs of Eq.40 and solve the self-consistency equation for $T = 0$. One finds the next solution:

$$\begin{aligned} \langle S_{\mathbf{k}}^z S_{\mathbf{k}'}^z \rangle_C &= -\langle \eta_{\mathbf{k}}^x \eta_{\mathbf{k}'}^y \eta_{\mathbf{k}}^y \eta_{\mathbf{k}'}^x \rangle_C \\ &= \frac{V_{\mathbf{k}}}{8} \frac{N\delta_{\mathbf{k},-\mathbf{k}'}}{B - \frac{V_{\mathbf{k}}}{2} + \sqrt{B^2 - BM_x V_{\mathbf{k}}}} \end{aligned} \quad (48)$$

Eq.48 corresponds to the lowest order solution for the spin-spin correlation and is valid within the paramagnetic region of the phase diagram. As expected to lowest order, the divergence happens at the uncorrelated critical

point $B_c = V_0/2$ (which is correct in 1D, and therefore should not display the instability previously found for the RPA, due to the shift of the Curie temperature); however this divergence shows an important difference with the one obtained in the classical Ising model (Eq.20): the non-commutativity of the interaction and transverse field terms in the Hamiltonian produce the square root term in the denominator of Eq.48, which modifies the scaling properties near the critical point. To see this explicitly, we consider the long wavelength limit of Eq.48, as a function of the reduced field $b = (B - B_c)/B_c$:

$$\langle S_{\mathbf{k}}^z S_{-\mathbf{k}}^z \rangle_C = \frac{1/4}{b + \frac{V_{\mathbf{k}}^2}{2B_c} + \sqrt{b+1}\sqrt{b + \frac{V_{\mathbf{k}}^2}{2B_c}}} \quad (49)$$

Near $b \sim 0$, a change in the behavior of interspin correlations from $(b + \frac{V_{\mathbf{k}}^2}{2B_c})^{-1}$ to $(b + \frac{V_{\mathbf{k}}^2}{2B_c})^{-1/2}$ will happen for $k^2 \sim 2bB_c/V$. The Fourier transform to position space is in this case proportional to the Bessel function of the second kind $K_0(\sqrt{2b}|r|)$, which displays the required asymptotic behavior for interspin correlations $\sim e^{\sqrt{2b}|r|}$ at large distances. The difference will be relevant when the distance is of the order of the inverse correlation length $|r| \sim \sqrt{b}$ only. The correlation length near the critical point scales as $\xi \sim b^{-1/2}$, and we obtain the critical exponent $\nu = 1/2$, as in the model without transverse field; however, the anomalous dimension obtained at the critical point is:

$$\langle S_{\mathbf{k}}^z S_{-\mathbf{k}}^z \rangle_C \sim \frac{1}{\sqrt{k^2}} \rightarrow \eta = 1 \quad (50)$$

This shows that with this method, the perturbative solution over the uncorrelated solution already captures a difference in the anomalous dimension between the phase transition driven by quantum fluctuations and the one driven by thermal fluctuations. Unfortunately we cannot derive an analytical formula for the scaling of the magnetization near B_c , because Eq.48 applies to the PM phase only, where the order parameter vanishes.

Now one can insert Eq.48 into Eq.41. As previously discussed, this approximation can fail when correlations are strong and induce an instability of the critical point. However in this case we know that the $T = 0$ critical point in 1D is correct, and therefore the approximation should be reliable. One obtains:

$$\lambda(\omega) = \frac{\omega}{2\pi} \int_{-\pi}^{\pi} \frac{\left(\frac{V_{\mathbf{q}}}{2}\right)^2 (B + \Omega_{\mathbf{q}}) d\mathbf{q}}{\left(B - \frac{V_{\mathbf{q}}}{2} + \Omega_{\mathbf{q}}\right) (\omega^2 - \Omega_{\mathbf{q}}^2)} \quad (51)$$

where $\Omega_{\mathbf{q}} = \sqrt{B^2 - BM_x V_{\mathbf{q}}}$ and we have taken the continuum limit. Adding an infinitesimal complex part $\omega \rightarrow \omega \pm i\epsilon$ the self-energy can then be calculated by contour integral methods. However, one must notice that the square root dependence introduces branch cuts which need to be accounted for. Hence, as we are mostly

interested in the frequency dependence, and the condition $B > B_c$ removes any divergences coming from $B - \frac{V_q}{2} + \Omega_q$, the final expression, to lowest order in B/V for the integrand $V_q^2 (B + \Omega_q) / \left(B - \frac{V_q}{2} + \Omega_q \right)$, should be a good approximation far from the critical point. The self-energy is then approximated by:

$$\lambda(\omega) \simeq \omega \frac{B^2 - \omega^2}{4B^2 M_x^2} - \frac{\omega (B^2 - \omega^2)^2 \text{sign}(B - |\omega|)}{4B^2 M_x^2 \sqrt{(B^2 - \omega^2)^2 - 4B^2 V^2 M_x^2}} \quad (52)$$

Eq.52 displays a rich structure as a function of frequency. The spectral density changes from the two initial poles $\omega = \pm B$ obtained in absence of correlations, to a combination of isolated poles and a continuum density of states, once the correlations are added. Also, at the large field fixed point $B \gg V$, the self-energy tends to zero and the two poles found in absence of correlations are recovered, as one would expect. This final result fully characterizes the solution for $\hat{G}(\omega)$, and shows how different approximations can be used on the hierarchy of correlations to obtain non-perturbative, analytical results.

V. CONCLUSIONS

We have studied the Ising model using the equation of motion technique and a decoupling scheme based on the scaling of spatial correlations between spins. We have shown that this method allows for a general approach to spin systems, which is not restricted to Ising models only. Furthermore, a similar approach would apply for the case of fermionic and bosonic systems as well. For the case of spin systems, the formalism is specially simple in terms of double-time Green's functions and Majorana fermions, but it can be applied to different spin representations such as the Holstein-Primakoff, hardcore bosons, fermionic, etc, without any difficulties. One of the advantages is that it allows to discuss systems in different dimensions and with a large variety of interactions. The only changes will be in the scaling properties of the hierarchy (its convergence) and the numerical integration in

the self-consistency equations. Importantly, the double-time formalism can be applied to out-of-time correlators as well³¹, which expands the possibilities of this method to study dynamical properties as well.

Regarding the specific models studied in this work, our results show that the Ising model in absence of a transverse field can be solved exactly to \mathcal{Z}^{-1} order. This already provides interesting results, even in 1D where we expect the hierarchy to be less accurate due to the small coordination number. We demonstrate the absence of a phase transition in 1D, and predict the value of the spin-spin correlation function $\langle S_{\mathbf{q}}^z S_{-\mathbf{q}}^z \rangle_C$ and of the energy of the ground state E_0 (Fig.4). Importantly, Eqs.29,30 and 31 correspond to a generalization of the widely used mean-field equations for the magnetization, now including two-body correlations. They are valid in arbitrary dimension and allow to characterize the phase diagram and the critical exponents. In addition, we have also shown how one can recover the well known Ginzburg-Landau critical exponents from the perturbative solution to lowest order.

When the transverse field is non-vanishing, the equations of motion for the Green's functions still can be solved analytically, but their self-consistency equations are more complicated and require numerical approaches. In general, one finds the appearance of dispersive collective modes (magnons) and branch cuts in the spectrum. An interesting difference, that appears to lowest order in perturbations, is that the critical exponent $\eta \neq 0$ at the quantum critical point. This stresses the difference with other methods that would just give the mean field value $\eta = 0$. We have shown that interactions in the quantum Ising model lead, in general, to a complicated expression for the self-energy including damping, and that the quasiparticle picture becomes just an approximate one. To show this explicitly we have approximated the behavior of the self-energy within the paramagnetic phase; it shows a rich behavior as a function of frequency, where discrete and continuum excitations are present.

We would like to acknowledge P.C.E. Stamp, T. Cox, and R. McKenzie for useful discussions. This work was supported by NSER of Canada.

¹ A. Dutta et al., *Quantum Phase Transitions in Transverse Field Spin Models: From Statistical Physics to Quantum Information*, Cambridge University Press, 2015.

² D. Sherrington and S. Kirkpatrick, Phys. Rev. Lett. **35**, 1792 (1975).

³ R. R. P. Singh and S. Chakravarty, Phys. Rev. Lett. **57**, 245 (1986).

⁴ R. Moessner and S. L. Sondhi, Phys. Rev. B **63**, 224401 (2001).

⁵ J. A. Kjall, J. H. Bardarson, and F. Pollmann, Phys. Rev. Lett. **113**, 107204 (2014).

⁶ P. B. Chakraborty, P. Henelius, H. Kjonsberg, A. W. Sandvik, and S. M. Girvin, Phys. Rev. B **70**, 144411 (2004).

⁷ M. Schechter and P. C. E. Stamp, Phys. Rev. B **78**, 054438 (2008).

⁸ F. Barahona, J. Phys. A: Math. Gen. **15**, 3241 (1982).

⁹ S. Boixo et al., Nature Physics **10**, 218 (2014).

¹⁰ L. Lamata et al., Nature **534**, 222 (2016).

¹¹ G. De las Cuevas and T. S. Cubitt, Science **351**, 1180 (2016).

¹² V. M. Bastidas, C. Emary, G. Schaller, and T. Brandes, Phys. Rev. A **86**, 063627 (2012).

¹³ A. Gómez-León and P. C. E. Stamp, Phys. Rev. B **95**, 054402 (2017).

¹⁴ N. Prokof'ev and P. Stamp, Reports on Progress in Physics **669** (2000).

- ¹⁵ P. Werner, K. Völker, M. Troyer, and S. Chakravarty, Phys. Rev. Lett. **94**, 047201 (2005).
- ¹⁶ M. Foss-Feig, K. R. A. Hazzard, J. J. Bollinger, and A. M. Rey, Phys. Rev. A **87**, 042101 (2013).
- ¹⁷ D. N. Zubarev, Soviet Physics Uspekhi **3**, 320 (1960).
- ¹⁸ Y. Nagaoka, Phys. Rev. **138**, A1112 (1965).
- ¹⁹ H.-Y. Wang, Z.-H. Dai, P. Fröbrich, P. J. Jensen, and P. J. Kuntz, Phys. Rev. B **70**, 134424 (2004).
- ²⁰ J. Schreiber, Physica B+C **96**, 27 (1979).
- ²¹ Á. Gómez-León, Phys. Rev. B **94**, 035144 (2016).
- ²² W. Mao, P. Coleman, C. Hooley, and D. Langreth, Phys. Rev. Lett. **91**, 207203 (2003).
- ²³ A. Shnirman and Y. Makhlin, Phys. Rev. Lett. **91**, 207204 (2003).
- ²⁴ S. Suzuki, J. ichi Inoue, and B. K. Chakrabarti, *Quantum Ising Phases and Transitions in Transverse Ising Models*, Springer, 2013.
- ²⁵ N. D. Mermin and H. Wagner, Phys. Rev. Lett. **17**, 1133 (1966).
- ²⁶ J. A. Cuesta and A. Sánchez, Journal of Statistical Physics **115**, 869 (2004).
- ²⁷ B. Braierr-Orrs, M. Weyrauch, and M. V. Rakov, Arxiv:1508.06508 (2015).
- ²⁸ J. A. Hertz, Phys. Rev. B **14**, 1165 (1976).
- ²⁹ M. L. Bellac, F. Mortessagne, and G. G. Batrouni, *Equilibrium and Non-Equilibrium Statistical Thermodynamics*, Cambridge University Press, 2004.
- ³⁰ W. H. Dickhoff and D. V. Neck, *Many-Body Theory Exposed!*, World Scientific Publishing, 2005.
- ³¹ J. H. H. Perk and H. Au-Yang, Journal of Statistical Physics **135**, 599 (2009).

Appendix A: Correlated part of the 4-point function

Here we include the details for the calculation of the 4-point function $G_{ppn,n}^{xy\alpha,\beta}(t,t') = -i\langle\eta_p^x(t)\eta_p^y(t)\eta_n^\alpha(t);\eta_n^\beta(t')\rangle$. The general equation of motion for $p \neq n$ is:

$$\omega G_{ppn,n}^{\mu\nu\alpha,\beta} = \frac{1}{2\pi}\langle\{\eta_p^\mu\eta_p^\nu\eta_n^\alpha,\eta_n^\beta\}\rangle + i\langle[H,\eta_p^\mu\eta_p^\nu\eta_n^\alpha];\eta_n^\beta\rangle \quad (\text{A1})$$

As we are interested in the correlated part of the Green's function we must remove the equation of motion for the uncorrelated part $\mathcal{G}_{ppn,n}^{\mu\nu\alpha,\beta} = G_{ppn,n}^{\mu\nu\alpha,\beta} - \langle\eta_p^\mu\eta_p^\nu\rangle G_{n,n}^{\alpha,\beta}$:

$$\begin{aligned} \omega\mathcal{G}_{ppn,n}^{\mu\nu\alpha,\beta} &= \epsilon_{x\alpha\theta}iB(G_{ppn,n}^{\mu\nu\theta,\beta} - \langle\eta_p^\mu\eta_p^\nu\rangle G_{n,n}^{\theta,\beta}) + iB(\epsilon_{x\mu\theta}G_{ppn,n}^{\theta\nu\alpha,\beta} + \epsilon_{x\nu\theta}G_{ppn,n}^{\mu\theta\alpha,\beta}) \\ &+ \epsilon_{z\alpha\theta}\sum_{i\neq n}V_{n,i}\left(G_{ppi,n}^{\mu\nu xy\theta,\beta} - \langle\eta_p^\mu\eta_p^\nu\rangle G_{iin,n}^{xy\theta,\beta}\right) + \sum_{i\neq p}V_{p,i}\left(\epsilon_{z\mu\theta}G_{iipn,n}^{xy\theta\nu\alpha,\beta} + \epsilon_{z\nu\theta}G_{iipn,n}^{xy\mu\theta\alpha,\beta}\right) \end{aligned} \quad (\text{A2})$$

Then, we make use of the conservation law $\partial_t\langle\eta_p^\mu\eta_p^\nu\rangle = 0$ and expand in correlations (neglecting \mathcal{Z}^{-2} order terms), finding:

$$\begin{aligned} \omega\mathcal{G}_{ppn,n}^{\mu\nu\alpha,\beta} &= iB(\epsilon_{x\alpha\theta}\mathcal{G}_{ppn,n}^{\mu\nu\theta,\beta} + \epsilon_{x\mu\theta}\mathcal{G}_{ppn,n}^{\theta\nu\alpha,\beta} + \epsilon_{x\nu\theta}\mathcal{G}_{ppn,n}^{\mu\theta\alpha,\beta}) \\ &+ \epsilon_{z\alpha\theta}\sum_{i\neq n,p}V_{n,i}(\langle\eta_p^\mu\eta_p^\nu\eta_i^x\eta_i^y\rangle_C G_{n,n}^{\theta,\beta} + \langle\eta_i^x\eta_i^y\rangle\mathcal{G}_{ppn,n}^{\mu\nu\theta,\beta}) \\ &+ \epsilon_{z\alpha\theta}V_{n,p}(\langle\eta_p^\mu\eta_p^\nu\eta_p^x\eta_p^y\rangle - \langle\eta_p^\mu\eta_p^\nu\rangle\langle\eta_p^x\eta_p^y\rangle)G_{n,n}^{\theta,\beta} \\ &+ \epsilon_{z\mu\theta}\sum_{i\neq p,n}V_{p,i}(\langle\eta_i^x\eta_i^y\rangle\mathcal{G}_{ppn,n}^{\theta\nu\alpha,\beta} + \langle\eta_p^\theta\eta_p^\nu\rangle\mathcal{G}_{iin,n}^{xy\alpha,\beta}) \\ &+ \epsilon_{z\nu\theta}\sum_{i\neq p,n}V_{p,i}(\langle\eta_i^x\eta_i^y\rangle\mathcal{G}_{ppn,n}^{\mu\theta\alpha,\beta} + \langle\eta_p^\mu\eta_p^\theta\rangle\mathcal{G}_{iin,n}^{xy\alpha,\beta}) \\ &+ V_{p,n}(\epsilon_{z\mu\theta}\langle\eta_p^\theta\eta_p^\nu\rangle + \epsilon_{z\nu\theta}\langle\eta_p^\mu\eta_p^\theta\rangle)(G_{nnn,n}^{xy\alpha,\beta} - \langle\eta_n^x\eta_n^y\rangle G_{n,n}^{\alpha,\beta}) \end{aligned} \quad (\text{A3})$$

Importantly, if we make use of the properties of the transverse Ising model $\langle S_i^y \rangle = 0$ and $\langle S_i^z S_j^y \rangle = 0$, we can simplify the different concrete cases. Also, the Green's function $G_{nnn,n}^{xy\alpha,\beta}$ appear in the equation of motion, but fortunately it can be calculated exactly:

$$G_{nnn,n}^{xyz,\beta} = \frac{1}{2\pi\omega}(\delta_{x,\beta}\langle\eta_n^y\eta_n^z\rangle - \delta_{y,\beta}\langle\eta_n^x\eta_n^z\rangle + \delta_{z,\beta}\langle\eta_n^x\eta_n^y\rangle) \quad (\text{A4})$$

Appendix B: Classical Ising model

The full equation of motion in momentum space is given by:

$$\omega G_{\mathbf{k}}^{\alpha,\beta} = \frac{N}{2\pi} \delta(\mathbf{k}) \delta_{\alpha,\beta} + iB\epsilon_{x\alpha\mu} G_{\mathbf{k}}^{\mu,\beta} + \epsilon_{z\alpha\mu} iM_z V_0 G_{\mathbf{k}}^{\mu,\beta} + \epsilon_{z\alpha\mu} \frac{1}{N} \sum_{\mathbf{q}} V_{\mathbf{q}} \mathcal{G}_{\mathbf{q},\mathbf{k}-\mathbf{q}}^{xy\mu,\beta} \quad (\text{B1})$$

Neglecting the transverse term and writing the different components in matrix form we find:

$$\begin{pmatrix} \omega & -iM_z V_0 \\ iM_z V_0 & \omega \end{pmatrix} \begin{pmatrix} G_{\mathbf{k}}^{x,\beta} \\ G_{\mathbf{k}}^{y,\beta} \end{pmatrix} = N \frac{\delta_{\mathbf{k},0}}{2\pi} \begin{pmatrix} \delta_{x,\beta} \\ \delta_{y,\beta} \end{pmatrix} + \frac{1}{N} \sum_{\mathbf{q}} V_{\mathbf{q}} \begin{pmatrix} \mathcal{G}_{\mathbf{q},\mathbf{k}-\mathbf{q}}^{xyy,\beta} \\ -\mathcal{G}_{\mathbf{q},\mathbf{k}-\mathbf{q}}^{xyx,\beta} \end{pmatrix} \quad (\text{B2})$$

Solving the equation of motion for the correlated part and assuming that the magnetization is homogeneous we find:

$$\begin{aligned} \mathcal{G}_{\mathbf{k},\mathbf{k}'}^{xyx,\beta} &= V_{\mathbf{k}'} \frac{N\delta_{\mathbf{k},-\mathbf{k}'} \left(\frac{1}{4} - M_z^2 \right) - \langle \eta_{\mathbf{k}}^x \eta_{\mathbf{k}}^y \eta_{\mathbf{k}'}^x \eta_{\mathbf{k}'}^y \rangle_C}{\omega^2 - V_0^2 M_z^2} \left(iV_0 M_z G_0^{x,\beta} - \omega G_0^{y,\beta} \right) \\ \mathcal{G}_{\mathbf{k},\mathbf{k}'}^{xyy,\beta} &= V_{\mathbf{k}'} \frac{N\delta_{\mathbf{k},-\mathbf{k}'} \left(\frac{1}{4} - M_z^2 \right) - \langle \eta_{\mathbf{k}}^x \eta_{\mathbf{k}}^y \eta_{\mathbf{k}'}^x \eta_{\mathbf{k}'}^y \rangle_C}{\omega^2 - V_0^2 M_z^2} \left(iV_0 M_z G_0^{y,\beta} + \omega G_0^{x,\beta} \right) \end{aligned}$$

where $G_{\mathbf{k}}^{\alpha,\beta} = G_0^{\alpha,\beta} \delta(\mathbf{k}) / N$. Then we can rewrite the initial equation of motion as:

$$\left(\omega - \hat{H}_0 \right) \hat{G} = \frac{\hat{\delta}}{2\pi} + \hat{\Sigma}(\omega) \cdot \hat{G} \quad (\text{B3})$$

being $\hat{G} = \begin{pmatrix} G_0^{x,\beta} \\ G_0^{y,\beta} \end{pmatrix}$, $\hat{\delta} = \begin{pmatrix} \delta_{x,\beta} \\ \delta_{y,\beta} \end{pmatrix}$, $\hat{H}_0 = \begin{pmatrix} 0 & iM_z V_0 \\ -iM_z V_0 & 0 \end{pmatrix}$, $\hat{G}^{(0)} = \left(\omega - \hat{H}_0 \right)^{-1} \cdot \hat{\delta}$ and

$$\hat{\Sigma}(\omega) = \lambda(\omega) \begin{pmatrix} \omega & iV_0 M_z \\ -iV_0 M_z & \omega \end{pmatrix} \quad (\text{B4})$$

$$\begin{aligned} \lambda(\omega) &= \frac{1}{N} \sum_{\mathbf{q}} |V_{\mathbf{q}}|^2 \frac{\frac{1}{4} - M_z^2 - \frac{1}{N} \langle \eta_{\mathbf{q}}^x \eta_{\mathbf{q}}^y \eta_{-\mathbf{q}}^x \eta_{-\mathbf{q}}^y \rangle_C}{\omega^2 - V_0^2 M_z^2} \\ &= \frac{\chi}{\omega^2 - V_0^2 M_z^2} \quad (\text{B5}) \end{aligned}$$

where $\chi = \frac{1}{N} \sum_{\mathbf{q}} |V_{\mathbf{q}}|^2 \left[\frac{1}{4} - M_z^2 - \frac{1}{N} \langle \eta_{\mathbf{q}}^x \eta_{\mathbf{q}}^y \eta_{-\mathbf{q}}^x \eta_{-\mathbf{q}}^y \rangle_C \right]$. Note that this previous expression indicates that a full solution requires to calculate χ later on, in a self-consistent way. The solution for the Green's function is easily found to be:

$$\hat{G} = \left(\omega - \hat{H}_0 - \hat{\Sigma}(\omega) \right)^{-1} \cdot \frac{\hat{\delta}}{2\pi} \quad (\text{B6})$$

with poles at:

$$\omega_i = \pm M_z V_0 \pm \sqrt{\chi} \quad (\text{B7})$$

Then we calculate the self-consistency equations for the magnetization and the interspin correlations. For the magnetization we find:

$$M_z = \frac{1}{2} \frac{\sinh\left(\frac{M_z V_0}{T}\right)}{\cosh\left(\frac{M_z V_0}{T}\right) + \cosh\left(\frac{\sqrt{\chi}}{T}\right)} \quad (\text{B8})$$

To correctly determine χ we need to first find a self-consistency equation for $\langle \eta_{\mathbf{q}}^x \eta_{\mathbf{q}}^y \eta_{-\mathbf{q}}^x \eta_{-\mathbf{q}}^y \rangle_C$, which is obtained from the expression for $\mathcal{G}_{\mathbf{q},-\mathbf{q}}^{xyx,y}$. We find:

$$-\langle \eta_{\mathbf{q}}^x \eta_{\mathbf{q}}^y \eta_{-\mathbf{q}}^x \eta_{-\mathbf{q}}^y \rangle_C = V_{-\mathbf{q}} \frac{N \left(\frac{1}{4} - M_z^2 \right) - \langle \eta_{\mathbf{q}}^x \eta_{\mathbf{q}}^y \eta_{-\mathbf{q}}^x \eta_{-\mathbf{q}}^y \rangle_C}{2\sqrt{\chi} \left[\cosh\left(\frac{M_z V_0}{T}\right) + \cosh\left(\frac{\sqrt{\chi}}{T}\right) \right]} \sinh\left(\frac{\sqrt{\chi}}{T}\right)$$

which corresponds to :

$$\langle \eta_{\mathbf{q}}^x \eta_{\mathbf{q}}^y \eta_{-\mathbf{q}}^x \eta_{-\mathbf{q}}^y \rangle_C = - \frac{N \left(\frac{1}{4} - M_z^2 \right) V_{-\mathbf{q}} \sinh \left(\frac{\sqrt{\chi}}{T} \right)}{2\sqrt{\chi} \left[\cosh \left(\frac{M_z V_0}{T} \right) + \cosh \left(\frac{\sqrt{\chi}}{T} \right) \right] - V_{-\mathbf{q}} \sinh \left(\frac{\sqrt{\chi}}{T} \right)} \quad (\text{B9})$$

Note that it nicely agrees with the lowest order, perturbative solution $\langle \eta_{\mathbf{q}}^x \eta_{\mathbf{q}}^y \eta_{-\mathbf{q}}^x \eta_{-\mathbf{q}}^y \rangle_c = \frac{-N \left(\frac{1}{4} - M_z^2 \right) V_{-q}}{4T \cosh^2 \left(\frac{V_0 M_z}{2T} \right) - V_{-q}}$ if we expand to linear order in χ . To finally obtain the self-consistency equation for χ , we insert the previous result into $\chi = \frac{1}{N} \sum_{\mathbf{q}} |V_{\mathbf{q}}|^2 \left[\frac{1}{4} - M_z^2 - \frac{1}{N} \langle \eta_{\mathbf{q}}^x \eta_{\mathbf{q}}^y \eta_{-\mathbf{q}}^x \eta_{-\mathbf{q}}^y \rangle_C \right]$, and get:

$$\chi = \left(\frac{1}{4} - M_z^2 \right) \frac{1}{N} \sum_{\mathbf{q}} \frac{2\sqrt{\chi} \left[\cosh \left(\frac{M_z V_0}{T} \right) + \cosh \left(\frac{\sqrt{\chi}}{T} \right) \right] |V_{\mathbf{q}}|^2}{2\sqrt{\chi} \left[\cosh \left(\frac{M_z V_0}{T} \right) + \cosh \left(\frac{\sqrt{\chi}}{T} \right) \right] - V_{-\mathbf{q}} \sinh \left(\frac{\sqrt{\chi}}{T} \right)} \quad (\text{B10})$$

which correctly agrees with the RPA result to linear order in χ . In the 1D case one can obtain an exact expression for the integral:

$$\int_{-\pi}^{\pi} \frac{dq}{2\pi} \frac{\cos^2(q)}{m - \cos(q)} = \frac{m\theta(m-1)}{m^2 - 1 + m\sqrt{m^2 - 1}} - m\theta(1-m)$$

where we have computed its value for $m > 1$ by contour integral in the complex plane, and to extend the result to $m < 1$, we have ‘‘regularized’’ the integral by calculating its principal value, deforming the unit circle around the poles. The final result is

$$\chi \stackrel{1D}{=} \left(\frac{1}{4} - M_z^2 \right) V_0^2 m^2 \left(\frac{\theta(m-1)}{m^2 - 1 + m\sqrt{m^2 - 1}} - \theta(1-m) \right) \quad (\text{B11})$$

being $m = 2\sqrt{\chi} \frac{\cosh \left(\frac{M_z V_0}{T} \right) + \cosh \left(\frac{\sqrt{\chi}}{T} \right)}{V_0 \sinh \left(\frac{\sqrt{\chi}}{T} \right)}$. The last important result is the calculation of the average energy, which in case of different possible solutions, will determine the ground state. The energy per spin of the ground state is:

$$\frac{E_0}{N} = \frac{\langle H \rangle}{N} = -\frac{1}{N} \sum_{i,j>i} V_{i,j} \langle S_i^z S_j^z \rangle \quad (\text{B12})$$

In the Majorana representation, the energy per spin becomes:

$$\frac{E_0}{N} = \frac{1}{N} \sum_{i,j>i} V_{i,j} \langle \eta_i^x \eta_i^y \eta_j^x \eta_j^y \rangle \quad (\text{B13})$$

$$= V_0 \langle \eta^x \eta^y \rangle^2 + \frac{1}{N} \sum_{\mathbf{q}} V_{\mathbf{q}} \langle \eta_{\mathbf{q}}^x \eta_{\mathbf{q}}^y \eta_{-\mathbf{q}}^x \eta_{-\mathbf{q}}^y \rangle_c \quad (\text{B14})$$

where in the second line we have separated into uncorrelated and correlated parts, and assumed homogeneous magnetization. The magnetization is obtained from the solution of the self-consistency equation, and the last term can be related with the two-point function as:

$$\frac{E_0}{N} = V_0 \langle \eta^x \eta^y \rangle^2 + i \int_{-\infty}^{\infty} \frac{\omega G_0^{y,y}(\omega \pm i\eta) + iV_0 M_z G_0^{x,y}(\omega \pm i\eta)}{e^{\beta\omega} + 1} d\omega \quad (\text{B15})$$

resulting in

$$\frac{E_0}{N} = -V_0 M_z^2 - \frac{1}{2} \frac{\sqrt{\chi} \sinh \left(\frac{\sqrt{\chi}}{T} \right)}{\cosh \left(\frac{M_z V_0}{T} \right) + \cosh \left(\frac{\sqrt{\chi}}{T} \right)} \quad (\text{B16})$$